



## Experiment Report Form

**The double page inside this form is to be filled in by all users or groups of users who have had access to beam time for measurements at the ESRF.**

Once completed, the report should be submitted electronically to the User Office using the **Electronic Report Submission Application:**

*<http://193.49.43.2:8080/smis/servlet/UserUtils?start>*

### ***Reports supporting requests for additional beam time***

Reports can now be submitted independently of new proposals – it is necessary simply to indicate the number of the report(s) supporting a new proposal on the proposal form.

The Review Committees reserve the right to reject new proposals from groups who have not reported on the use of beam time allocated previously.

### ***Reports on experiments relating to long term projects***

Proposers awarded beam time for a long term project are required to submit an interim report at the end of each year, irrespective of the number of shifts of beam time they have used.

### ***Published papers***

All users must give proper credit to ESRF staff members and proper mention to ESRF facilities which were essential for the results described in any ensuing publication. Further, they are obliged to send to the Joint ESRF/ ILL library the complete reference and the abstract of all papers appearing in print, and resulting from the use of the ESRF.

Should you wish to make more general comments on the experiment, please note them on the User Evaluation Form, and send both the Report and the Evaluation Form to the User Office.

### **Deadlines for submission of Experimental Reports**

- 1st March for experiments carried out up until June of the previous year;
- 1st September for experiments carried out up until January of the same year.

### **Instructions for preparing your Report**

- fill in a separate form for each project or series of measurements.
- type your report, in English.
- include the reference number of the proposal to which the report refers.
- make sure that the text, tables and figures fit into the space available.
- if your work is published or is in press, you may prefer to paste in the abstract, and add full reference details. If the abstract is in a language other than English, please include an English translation.



	<b>Experiment title:</b> Zinc electrodeposition from ionic liquids	<b>Experiment number:</b> SI-1827
<b>Beamline:</b> ID32	<b>Date of experiment:</b> from: 03.09.2008 to: 09.09.2008	<b>Date of report:</b> 13.02.2009
<b>Shifts: 18</b>	<b>Local contact(s):</b> Dr. Jerome Roy	<i>Received at ESRF:</i>
<b>Names and affiliations of applicants (* indicates experimentalists):</b> <b>Dr. Frank Uwe Renner*</b> <b>Dr. Dimitar Borissov*</b> <b>Dr. Michael Rohwerder*</b> <b>Dr. Aparna Pareek</b> <b>Dirk Vogel</b> <b>Max-Planck Institut für Eisenforschung, Düsseldorf, Germany</b>		

## Report:

The electrochemical deposition and re-dissolution of Zn on Au surface was investigated by in-situ surface X-ray diffraction, in order to understand the processes occurring at the Zn/metal electrochemical interface. The experiment was performed at the undulator beamline ID32 at the European Synchrotron Radiation Facility (ESRF).

## Experimental:

An Au single crystal with a polished (111) surface (MaTeck, Germany) was used as substrate for the experiment. For the in-situ diffraction studies, we used a portable electrochemical setup (TRECXI) [1] with an addition of a heating stage which allowed to heat the ionic liquid in UHV conditions. With this heating stage, it is also possible to perform electrodeposition at elevated temperatures around 130 °C. The electrochemical cell (EC) is encapsulated in a concentric capillary system, where the reference electrode (Pt wire) is inserted in the inner capillary, while the counter electrode (Pt wire) is wound around the inner capillary (Fig. 1c). With this setup, the electrolyte contact with the sample surface can be attained in the controlled gas atmosphere. Prior to the experiment, the Au (111) surface was prepared by few sputter-anneal cycles in UHV at the surface characterization lab of ID32. The surface quality of the sample was examined by Auger spectroscopy and LEED. The electrolyte comprises of ZnCl<sub>2</sub> and 1-Butyl-3-methylimidazolium Chloride ([BMIm]<sup>+</sup> Cl<sup>-</sup>) in 60:40 mol%. This ionic electrolyte is hygroscopic in nature and requires heating prior to the experiment to remove the absorbed water. Ionic liquid was heated in the portable chamber using a PCTFE container (Fig. 1a) for 12 hours in UHV (1×10<sup>-8</sup> mbar) up to 100 °C. The chamber was then filled with inert gas at ambient pressure and the electrochemical (capillary) cell was inserted by opening a UHV valve. The ionic liquid was pumped into the capillaries by using two syringes. The electrochemical cell was then separated from the rest of the chamber. and was evacuated to allow the sample transfer (Au (111))

crystal) from the UHV system. After the sample transfer, the portable chamber (TRECXI) was transported to the diffractometer. During the measurements, the portable chamber was again filled with the inert gas at ambient pressure to introduce the EC cell and a droplet of electrolyte at the end of the capillary was then brought into contact with the sample surface. Figure 1c shows a schematic of the electrochemical setup. This setup allows tracking the interface changes by in-situ x-ray diffraction without exposing the ionic liquid electrolyte and sample surface to ambient air.

The in-situ X-ray diffraction experiments were performed using a wavelength ( $\lambda$ ) of 0.539062 Å. The incident angle was chosen to 0.2°. The scattering vector  $\mathbf{q}$  is defined as  $\mathbf{q} = \mathbf{k}_f - \mathbf{k}_i$ , where  $\mathbf{k}_i$  and  $\mathbf{k}_f$  are the incoming and diffracted wave vectors, respectively. Au crystal possess a FCC unit cell (lattice parameters  $a_0 = 4.08$  Å,  $\alpha = \beta = \gamma = 90^\circ$ ), which can be transformed to a surface unit cell for Au (111) surface ( $\mathbf{a}_1 = \mathbf{a}_2 = \sqrt{2} \times a_0 = 5.767$  Å,  $\mathbf{a}_3 = \sqrt{3} \times a_0 = 7.064$  Å,  $\alpha = \beta = 90^\circ$ ,  $\gamma = 120^\circ$ ). This unit cell leads to a hexagonal reciprocal unit cell with lattice parameters  $\mathbf{a}_1^* = \mathbf{a}_2^* = 1.258$  Å,  $\mathbf{a}_3^* = 0.8895$  Å,  $\alpha = \beta = 90^\circ$ ,  $\gamma = 60^\circ$ . To describe the scattering vector  $\mathbf{q}$  and the reciprocal space of Au (111), we used the above mentioned reciprocal unit cell. The in-plane miller indices are then denoted by H & K, while L is the out-of plane index.

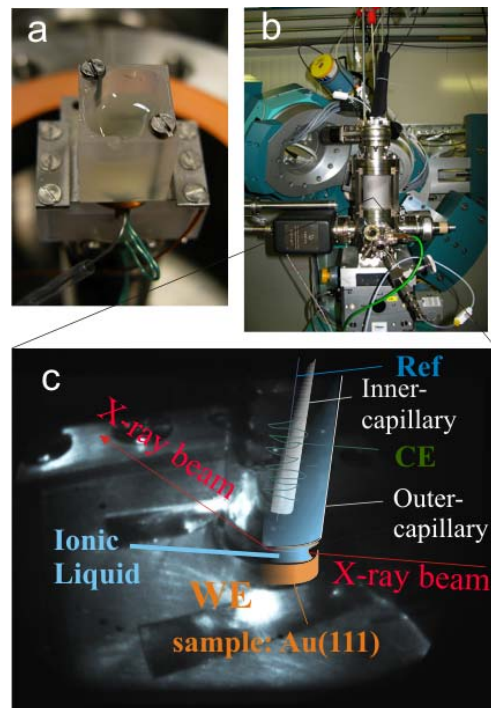


Figure 1: picture of the electrochemical setup used at the ESRF. a) The container half-filled with ionic liquid during heating. b) The portable EC cell-UHV chamber with the six-circle diffractometer. c) Schematic of the EC-cell explaining the experimental arrangement.

## Electrodeposition of epitaxially ordered Zn on Au (111) surface:

The electrodeposition was performed at the potential of -1.5 V. Figure 2 shows the first results of in-situ X-ray diffraction on Au (111) with Zn containing ionic liquid electrolyte. The sequence of in-plane scans measured in (1, 1) direction (with respect to time), after applying the potential are shown in Fig. 2. The in-plane scan measured directly after applying the potential (scan no. 1), shows only one reflection at  $H = K = 2$ , which corresponds to the Bragg reflection (2, 2, 0.05) of the Au substrate. With time (scan no. 2), additional in-plane intensity was observed at (2.16, 2.16, 0.05), which grows further (scans no. 2-5). The d-spacing for this reflection was calculated as 1.33 Å, which corresponds to the (11-20) Bragg reflection of Zinc. Furthermore, other than the pure Zn reflection, a new in-plane reflection developing at (2.06, 2.06, 0.05) was also observed, can be explained by the formation of  $\text{AuZn}_8$  alloy. These reflections show that the Zn and Zn-Au alloy are epitaxially ordered with respect to the Au (111) substrate. The Zn and Zn-Au alloy lattices are hexagonal closed packed lattice. Following the Zn-Au phase diagram [2], for lower Zinc concentrations the alloys possess cubic, tetragonal or orthorhombic structures ( $\alpha_{1-2}$ ,  $\alpha'_{1-2}$ ,  $\beta$ ,  $\beta_1$ ,  $\gamma$ ,  $\gamma_2$ ,  $\delta$ ), while for the Zn concentration greater than 75 at.% the alloys have hexagonal or hcp structure ( $\gamma_3$ ,  $\epsilon$ ). Figure 2a-d shows the out-of-plane and in-plane maps of the Au surface with Zn deposition, respectively. The out-of-plane maps (Fig. 2a & 2b) show the Zn and Zn-Au alloy peaks along with the Au substrate peak. The peaks are epitaxial and symmetrical arranged in reciprocal space. From the in-plane maps in (1, 1) direction, the gold and Zn peaks are clearly seen ( $\text{AuZn}_8$  and  $\text{Zn}\langle 11-20 \rangle \parallel \text{Au}\langle 220 \rangle$ ).

We also observed the formed pure Zn peak to get smaller with time, as can be seen from in-plane scan (scan no. 6) in Fig. 2. Here, the reflection corresponding to the  $\text{AuZn}_8$  alloy intense further, while intensity of the reflection corresponding to the pure Zn phase reduces. This observation indicates the pure Zn phase dissolves or transforms in an Au-Zn alloy; however, more experiments are required to corroborate this behavior.

The presented preliminary results of in-situ and ex-situ X-ray diffraction experiments suggest that during electrodeposition, a pure Zn film deposits first; but, as time elapses, an additional formation of a Zn-Au alloy is observed.

In conclusion, we observed the epitaxial growth of hexagonal Zn and  $\text{AuZn}_8$  on clean Au(111) surfaces, with the orientation  $\text{Zn}\langle 11-20 \rangle \parallel \text{Au}\langle 220 \rangle$ . The current investigation proves that the processes occurring at Au/Zn-IL electrochemical interfaces can be successfully probed to obtain detailed structural information during deposition.

Although the TREXCI setup provided the required inert gas atmosphere for these experiments, it still needs further modifications for our experiments. We could not obtain a CTR data set to assess the structural changes at the substrate-deposit interface after the Zn monolayer deposition, as the drop of ionic electrolyte was not stable on the Au substrate for long time. We are modifying the design of concentric capillary EC-cell for such purpose. In future, factors such as the presence of residual water/oxygen in the ionic electrolyte, influence of respective potential sequence in time, the surface roughness, will be further studied. Also, these experiments will be extended to more practical systems like Fe/Zn or Fe/Al.

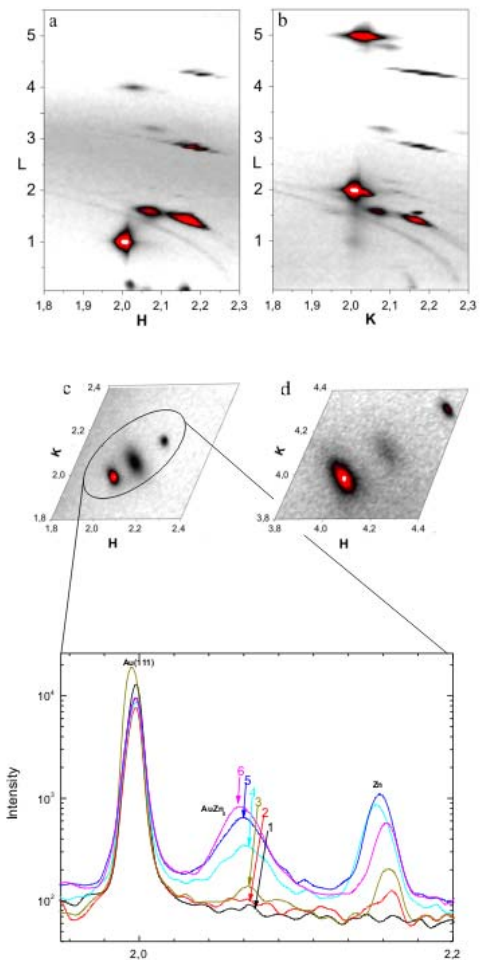


Figure 2: Data observed from the in-situ x-ray measurements. a) & b) Out-of-plane reciprocal space maps showing the Au substrate peak at (201), (022) and epitaxially ordered Zn and  $\text{AuZn}_8$  peaks along with their symmetrical equivalents. c) & d) In-plane maps in (1, 1) direction showing the three peaks of Au,  $\text{AuZn}_8$ , Zn peaks. Several in-plane scans

## References:

1. Renner, F. U.; Gründer, Y.; Zegenhagen, J.: Rev. Sci. Instrum., 78 (2007), 033903.
2. Okamoto, H.; Massalski, T. B.: Bulletin of Alloy Phase Diagrams, 10 (1989), 59.